THE JOURNAL OF BIOLOGICAL CHEMISTRY VOL. 285, NO. 1, pp. 409–421, January 1, 2010

Increased cAMP Levels Modulate Transforming Growth Factor-β/Smad-induced Expression of Extracellular Matrix Components and Other Key Fibroblast Effector Functions

Received for publication, June 30, 2009, and in revised form, October 23, 2009 Published, JBC Papers in Press, October 26, 2009, DOI 10.1074/jbc.M109.038620

Meinhard Schiller[‡1], Sylviane Dennler[§2], Ulf Anderegg[¶], Agatha Kokot[‡], Jan C. Simon[¶], Thomas A. Luger[‡], Alain Mauviel[§3], and Markus Böhm[‡4]

From the [‡]Department of Dermatology, Ludwig Boltzmann Institute for Cell Biology and Immunobiology of the Skin, 48149 Münster, Germany, [§]INSERM U697, Université Denis-Diderot, 75011 Paris, France, and the [¶]Department of Dermatology, Leipzig University Medical Center, 04103 Leipzig, Germany

cAMP is a key messenger of many hormones and neuropeptides, some of which modulate the composition of extracellular matrix. Treatment of human dermal fibroblasts with dibutyryl cyclic AMP and forskolin antagonized the inductive effects of transforming growth factor-β (TGF-β) on the expression of collagen, connective tissue growth factor, tissue inhibitor of matrix metalloproteinase-1, and plasminogen activator inhibitor type I, four prototypical TGF-β-responsive genes. Increased intracellular cAMP prevented TGF-β-induced Smad-specific gene transactivation, although TGF-β-mediated Smad phosphorylation and nuclear translocation remained unaffected. However, increased cAMP levels abolished TGF-β-induced interaction of Smad3 with its transcriptional co-activator cAMP-response element-binding protein (CREB)-binding protein (CBP)/p300. Overexpression of the transcriptional co-activator CBP/p300 rescued Smad-specific gene transcription in the presence of cAMP suggesting that sequestration of limited amounts of CBP/p300 by the activated cAMP/CREB pathway is the molecular basis of this inhibitory effect. These findings were extended by two functional assays. Increased intracellular cAMP levels suppressed the inductive activity of TGF-β to contract mechanically unloaded collagen lattices and resulted in an attenuation of fibroblast migration of mechanically induced cell layer wounds. Of note, cAMP and TGF-β synergistically induced hyaluronan synthase 2 (*HAS2*) expression and hyaluronan secretion, presumably via putative CREB-binding sites adjacent to Smad-binding sites within the *HAS2* promoter. Our findings identify the cAMP pathway as a potent but differential and promoter-specific regulator of TGF-β-mediated effects involved in extracellular matrix homeostasis.

The fibroblast is the most abundant cell type in normal connective tissues and plays a central role in the synthesis, degradation, and remodeling of extracellular matrix (ECM).[5] Consequently, increased activity and proliferation of resident fibroblasts are central to fibrosis in all tissues. Through their ability to modulate the expression of ECM components and ECM-degrading enzymes, cytokines, growth factors, hormones, neuropeptides, and environmental factors, such as ultraviolet light, fibroblasts orchestrate the balance between ECM destruction and neosynthesis (1–4). Disruption of the fragile equilibrium between anabolic and catabolic mediators may lead to excessive ECM deposition, the hallmark of fibrotic disorders such as liver cirrhosis, renal sclerosis, systemic sclerosis, and keloids. Among the mediators that influence ECM composition, transforming growth factor-β (TGF-β) turned out to be a crucial regulator of ECM neosynthesis, as it controls both the expression of components of the ECM network such as the fibrillar collagens and fibronectin, the expression of protease inhibitors, including plasminogen activator inhibitor-1 (PAI-1) or tissue inhibitor of metalloproteinases (5). These combined anabolic and anti-catabolic effects make TGF-β a key growth factor in the development of tissue fibrosis (6).

Cellular signaling from the TGF-β family of growth factors (*e.g.* activins, bone morphogenic proteins, and the TGF-β) is initiated by binding of the ligands to transmembrane receptor serine/threonine kinases, TβRI and TβRII. Following receptor activation, signaling from the cell surface to the nucleus occurs predominantly by phosphorylation of cytoplasmic mediators of the Smad family (7, 8). Briefly, the receptor-associated Smads (R-Smads), such as Smad1, Smad2, Smad3, and Smad5, interact directly with, and are phosphorylated by, activated type I receptors of the TGF-β superfamily. Activation of R-Smads is ligand-specific, but each of them forms, upon phosphorylation, heteromeric complexes with Smad4, which functions as a common mediator for all receptor-activated Smads. R-Smad-Smad4

[1] Recipient of Deutsche Forschungsgemeinschaft Postdoctoral Fellowship Schi 585/2-1. To whom correspondence may be addressed: University Hospital Münster, Dept. of Dermatology; Von-Esmarch-Str. 58, 48149 Münster, Germany. Tel.: 11-49-251-8356501; Fax: 11-49-251-8356522; E-mail: schillm@uni-muenster.de.

[2] Recipient of a postdoctoral fellowship from Institut National du Cancer and Région Ile-de-France.

[3] Supported by the Donation Henriette et Emile Goutière, Cancéropôle Ile-de-France, and INSERM, France. To whom correspondence may be addressed: INSERM U697, Hôpital Saint-Louis, 1 Ave. Claude Vellefaux, 75010 Paris, France. Tel.: 33-153-722-069; Fax: 33-153-722-051; E-mail: alain.mauviel@inserm.fr.

[4] Supported by grants from the Deutsche Forschungsgemeinschaft (DFG) BO 1075/ 5-1 and BO 1075/5-3.

[5] The abbreviations used are: ECM, extracellular matrix; CBP, CREB-binding protein; CRE, cAMP-response element; CREB, CRE-binding protein; CTGF, connective tissue growth factor; Bt_2cAMP, dibutyryl cyclic AMP; HDF, human dermal fibroblasts; HA, hyaluronan; PAI-1, plasminogen activator inhibitor-1; PKA, protein kinase A; TGF-β, transforming growth factor-β; FCS, fetal calf serum; ELISA, enzyme-linked immunosorbent assay; PICP, procollagen I C-terminal peptide; ERK, extracellular signal-regulated kinase; α-MSH, α-melanocyte-stimulating hormone; TβRI ,TGF-β receptor type I.

complexes are then translocated into the nucleus where they function as transcription factors, directly or in association with other DNA binding factors. Finally, inhibitory Smads, such as Smad6 or Smad7, interfere with TGF-β signaling by preventing R-Smad phosphorylation and subsequent nuclear translocation of R-Smad-Smad4 complexes (7, 8).

Several ECM-related genes have been identified as Smad targets, the only downstream substrates of TβRI known so far, including those encoding fibrillar collagens and TIMP1 (9), PAI-1 (10), connective tissue growth factor (CTGF) (11), and β5-integrin (12).

One signal transduction mediator that may interfere with TGF-β-initiated functions is cAMP. It transmits signals from a variety of hormones acting at the cell surface via guanine nucleotide-binding (G)-protein-coupled receptors to activate cAMP-dependent protein kinase A (PKA) (13). The balance between adenylate cyclase and cyclic nucleotide phosphodiesterase activities determines intracellular cAMP levels. In the basal state, PKA resides in the cytoplasm. cAMP induction liberates the catalytic subunits of PKA that then diffuse into the nucleus where they phosphorylate transcription factors, such as cAMP-response element-binding protein (CREB) (14). PKA phosphorylates CREB at serine 133, thereby allowing its association with the transcriptional co-activators CBP and p300 (15, 16). CREB transactivates cAMP-responsive genes by binding as a dimer to a conserved, 8-bp, palindromic cAMP-response element (CRE), TGACGTCA. Over 100 genes with functional CREs have been identified thus far (17).

It is reasonable to hypothesize that a better understanding of the mechanisms of TGF-β-mediated up-regulation of ECM gene expression in fibrotic tissue will provide novel approaches to the therapy of these diseases. Accordingly, deciphering of the mechanisms by which pro-inflammatory cytokines, hormones, and neuropeptides are able to interfere with the TGF-β-induced Smad signaling is of great importance.

In this study, we therefore focused on the effects of increased cAMP levels on key functions of dermal fibroblasts. We demonstrate an important role of cAMP in TGF-β-mediated expression of several ECM components and TGF-β-mediated effects such as wound closure and contraction.

EXPERIMENTAL PROCEDURES

Cell Culture and Biochemical Reagents—Human dermal fibroblasts (HDF) from neonatal foreskin were purchased from Cell Systems, St. Katharinen, Germany. The immortalized NIH3T3 fibroblast cell line derived from mouse embryos was a kind gift from Dr. Erwin F. Wagner (Institute for Molecular Pathology, Vienna, Austria). All fibroblasts were grown in Dulbecco's modified Eagle's medium supplemented with 10% heat-inactivated fetal calf serum (FCS), 2 mM glutamine, and antibiotics (100 units/ml penicillin, 50 mg/ml streptomycin-G, and 0.25 mg/ml Fungizone™) in a humidified atmosphere of 5% CO_2. Human recombinant TGF-β_1, purchased from R&D Systems, Inc. (Minneapolis, MN), referred to as TGF-β throughout the text, was used at a concentration of 10 ng/ml. Forskolin and dibutyryl-cAMP (Bt_2cAMP) were purchased from Sigma.

Plasmid Constructs—pCRE-luc (Mercury™ pathway luciferase system, Clontech) was used to determine CRE-driven transcription. The N-terminally FLAG-tagged Smad3 expression vector, a gift from A. Atfi, Paris, France, has been described previously (18). $(CAGA)_9$-luc, consisting of nine tandem repeats of the motif CAGA-binding Smad3 and Smad4, was used as a Smad3/Smad4-specific reporter (10). To measure prototypic TGF-β responses in the context of natural promoter sequences identified as Smad3 targets, we used p800-luc (a gift from D. J. Loskutoff, Scribbs Research Institute, San Diego), which contains 800 bp of human *PAI-1* promoter (10, 19) cloned upstream of the luciferase gene. The G5E1b-luc plasmid containing five GAL4-binding sites driving the expression of luciferase, the Gal4-Smad3 and VP16-CBP fusion protein expression vectors, VP16 empty vector, and p300 expression vector have been described before (20–22).

Transient Cell Transfections and Reporter Assays—For reporter assays, cells were seeded in 6- or 12-well plates and transfected at ~60–70% confluency with a liposome-based protocol (FuGENE™, Roche Diagnostics, or JetPEI™, Polyplus transfection, Illkirch, France). The total plasmid concentration was kept constant, and when needed, vector DNA was added. 0.2 μl of pRSV-β-galactosidase or 0.080 μg of pRL TK-luc (Fig. 4) was co-transfected in every experiment to monitor transfection efficiencies. Following incubation, cells were rinsed twice with phosphate-buffered saline, harvested by scraping, and lysed in commercial reporter lysis buffers (Promega Corp., Madison, WI). Luciferase and β-galactosidase activity were measured using corresponding assay kits (Promega, Madison, WI, and Roche Diagnostics, respectively).

Quantitative Real Time PCR—Total RNA was isolated from HDF using a commercial purification kit (Promega, Madison, WI). After DNA digestion, cDNA synthesis was done with oligo(dT) primers and RevertAid™ M-MuLV reverse transcriptase (Fermentas Life Sciences, Hanover, MD) according to the manufacturer's instructions. Quantitative real time PCR was performed in a total volume of 10 μl with SYBR Green PCR Master Mix (Applied Biosystems, Foster City, CA) and a 200 nM concentration of each primer. Primers were designed with the computer program Primer Express (Applied Biosystems), using parameters recommended by the manufacturer. Primer sequences were as follows: *PAI-1* (GenBank™ accession number NM_000602) 5′-AAT CAG ACG GCA GCA CTG TC-3′ (forward primer) and 5′-CTT TCC AGT GGC TGA TGA GC-3′ (reverse primer) resulting in a fragment of 219 bp; *COL1A1* (GenBank™ accession number NM_000088.3) 5′-CAG CCG CTT CAC CTA CAG-3′ (forward primer) and 5′-AAT CAC TGT CTT GCC CCA GG-3′ (reverse primer) resulting in a fragment of 72 bp; *COL1A2* (GenBank™ accession number NM_000089) 5′-AGC AAC ATG CCA ATC TTT ACA AGA G-3′ (forward primer) and 5′-ATC ATA CTG AGC AGC AAA GTT CCC-3′ (reverse primer) resulting in a fragment of 190 bp; *CTGF* (GenBank™ accession number NM_001901) 5′-AAT GAC AAC GCC TCC TGC AG-3′ (forward primer) and 5′-GCA GCC AGA AAG CTC AAA CTT G-3′ (reverse primer) resulting in a fragment of 153 bp, *TIMP1* (GenBank™ accession number NM_003254) 5′-TAC TTC CAC AGG TCC CAC AAC C-3′ (forward primer) and 5′-CAT TCC TCA CAG CCA ACA GTG TAG-3′ (reverse primer) resulting in a fragment of 167 bp; and *HAS2* (GenBank™

accession number NM_005328) 5′-GGA CGA CTT TAT GAC CAA GAG CTG-3′ (forward primer) and 5′-TGT GAT TCC AAG GAG GAG AGA GAC-3′ (reverse primer) resulting in a fragment of 110 bp. Reactions were carried out in an ABI-Prism 7000 sequence detector supplied with SDS 2.1 software (Applied Biosystems) in duplicate using the following conditions: an initial activation step consisted of 2 min at 50 °C, an single denaturation step consisted of 15 min at 95 °C, followed by 40 cycles of 15 s at 95 °C and 60 s at 60 °C, and a final cycle of 15 s at 95 °C, 15 s at 60 °C, and 15 s at 95 °C. Levels of gene expression in each sample were quantified using the $2^{-\Delta\Delta CT}$ method (after validation assays for each gene primer set) as described by Livak and Schmittgen (23), using *GAPDH* gene expression as endogenous control for *GAPDH* primers as follows: 5′-TGC ACC ACC AAC TGC TTA GC-3′ and 5′-GGC ATG GAC TGT GGT CAT GAG-3′. For each condition, the ground condition was set as 1. Expression of each gene was assessed by three independent PCR analyses. Significance of the data were determined by the Student's *t* test.

Determination of Procollagen I C-terminal Peptide—Amounts of procollagen I C-terminal peptide as a marker for procollagen I secretion were determined by a commercially available ELISA (Takara, Shiga, Japan). HDF were seeded into 12-well tissue culture plates at a density of 250,000 cells per well. Confluent HDF were then serum-starved for 2 days and subsequently stimulated with forskolin or Bt_2cAMP, TGF-β, or both agents in the presence of 50 μg/ml ascorbate. Culture supernatants were harvested after 48 h, centrifuged, and frozen at −70 °C until use. Statistical evaluation from triplicate wells was performed using the Student's *t* test.

Western Blotting—Subconfluent HDF were placed in fresh medium containing 1% FCS for 12–24 h before stimulation with various agents. The cells were washed with cold phosphate-buffered saline and lysed by addition of SDS lysis buffer (100 mM Tris-HCl (pH 6.8), 1% SDS, 0.1 M dithiothreitol, 0,1 mM orthovanadate) followed by boiling for 5 min. Proteins (50 μg/lane) were separated on 10 or 12% SDS-polyacrylamide gels and transferred to nitrocellulose Hybond ECL$^+$ (Amersham Biosciences). After blocking with 5% nonfat dry milk in 20 mM Tris (pH 7.6), 137 mM NaCl, and 0.1% Tween 20 for 1 h at room temperature, filters were incubated with either polyclonal anti-type I collagen (1:1000 dilution, Southern Biotech, Birmingham, AL), monoclonal C9 anti-PAI-1 (1:200 dilution, Santa Cruz Biotechnology, Santa Cruz, CA), anti-phospho-Smad3 (Ser-33/435) (1:1000, Calbiochem-Novabiochem), anti-Smad2/3 (1:500, BD Transduction Laboratories), anti-phospho-ERK1/ERK2 (Thr-202/Tyr-204) (1:1000, Cell Signaling Technology, Beverly, MA), monoclonal anti-tubulin (1:1000, Oncogene, San Diego), or monoclonal anti-actin (1:5000 dilution, Sigma) antibodies in blocking solution overnight at 4 °C. After three washes in 20 mM Tris (pH 7.6), 137 mM NaCl, 0.1% Tween 20, membranes were incubated with species-specific (anti-rabbit or anti-mouse) IgG-horseradish peroxidase-conjugated antibodies (1:5000 dilution) (Santa Cruz Biotechnology) in blocking solution for 1 h at room temperature. Membranes were then washed, and detection of immunoreactive proteins was performed with the ECL$^+$Plus chemiluminescent reagent according to the manufacturer's instructions (Amersham Biosciences). In some experiments, densitometric analysis was performed using the ImageQuant 5.0 software from GE Healthcare. All Western blots were repeated three times.

Immunofluorescence—HDF seeded into eight-well tissue chambers (Lab-Tek, Nalge Nunc International, Naperville, IL) were fixed with methanol for 30 min at −20 °C. Nonspecific binding was blocked with 5% goat/donkey serum for 1 h at room temperature. Endogenous Smad2/3 content was detected by incubation for 2 h at room temperature with a monoclonal anti-Smad2/3 antibody (1:250, BD Transduction Laboratories, Palo Alto, CA). After washing, bound antibodies were visualized by secondary rabbit anti-mouse IgG antibodies conjugated with Texas Red (1:800, Dianova, Hamburg, Germany). After three final washes, slides were counterstained with 4′,6-diamidino-2-phenylindole to visualize cell nuclei. After mounting, specimens were examined with a fluorescence microscope (Axioskop2, Zeiss, Germany) equipped with a digital camera. For negative controls, whole mouse serum was used instead of the primary antibody, or the primary antibody was omitted.

Collagen Matrix Contraction—NIH3T3 and HDF were harvested from monolayer culture with 0.25% trypsin and 1 mM EDTA, and then trypsin was neutralized with 1% FCS-containing medium. Collagen lattices in 60-mm dishes were prepared with 7 ml of a mixture containing 10^6 fibroblasts and 1 mg/ml native type I collagen (Biocoat^{TM}, BD Biosciences) in medium supplemented with 1% FCS. When needed, forskolin, Bt_2cAMP, and/or TGF-β were added to the mixture before polymerization of the collagen matrix. Polymerization of collagen matrices required 60 min at 37 °C. To initiate lattice contraction, freshly polymerized matrices were released from the underlying culture dish with a few gentle taps on the dish. The gels were then incubated at 37 °C in a 5% CO_2 atmosphere and photographed after 1–6 days, and the area of each gel was calculated using imaging software analysis. Data are expressed as the percentage of area compared with the original gel size.

Cell Migration Assays—A modified "scratch" migration assay was used for the assessment of the migration of fibroblasts as described previously for studying keratinocyte cell migration (24). HDF were seeded into 12-well tissue culture plates at a density of 200,000 cells per well and cultured until 95% confluent. A migration gap of ~0.8 mm was then created by introducing a scratch to the adherent layer of cultured cells using a sterile Gilson 200-μl pipette tip. The scratch was administered by hand using a sufficiently applied degree of pressure to remove adherent cells from the polystyrene substrate but not enough to cause physical damage to the polystyrene surface. The repeated nature of this procedure resulted in a cell-free gap of ~0.8 mm between two adjoining areas of fibroblasts at 90–95% confluence (see corresponding figures). At this point, cell culture medium was replaced two times with fresh medium to reduce the number of cells introduced into suspension reattaching to the cell-free zone during experimentation. Dishes were then incubated with Bt_2cAMP, forskolin, or TGF-β (alone or in combination) for 24–72 h in a 95% air, 5% CO_2 environment. Migration of the cells from the two regions of 90–95% adherent culture density into the cell-free zone was observed at a 24-, 48-, and 72-h time period and recorded by microscopy (Zeiss Axiovert 100, equipped with a digital camera).

Determination of Hyaluronan Secretion—The hyaluronan in fibroblast culture supernatants amounts was determined using an ELISA (Corgenix, Peterborough, UK) according to the manufacturer's instructions (sample dilution 1:10). ELISA readings were measured at an extinction of 450 nm with SynergyHT Reader and analyzed using the KC4-Pro Software (both Biotek, Bad Friedichshall, Germany).

In Silico Promoter Analysis—For bioinformatic analyses, the Genomatix software package (Genomatix Software, München, Germany) was used. Proximal promoter sequences (2 kb upstream and 0.2 kb downstream of the transcriptional start sites) were extracted with help of the ElDorado module (release 4.6). Identification of CREB and Smad3 transcription factor-binding sites in the sets of sequences was performed by using the MatInspector module of the Genomatix data base, which employed the Matrix Family Library version 7.1 (June 2008) (25). All analyses were conducted with high threshold values (core similarity 1.0, matrix similarity > 0.9).

RESULTS

CRE-dependent Response in HDF—We first analyzed the immediate consequences of increased intracellular cAMP levels by treating HDF with forskolin, a well established artificial activator of adenylate cyclase and an inducer of increased cAMP levels in these cells (26). As shown in Fig. 1*A*, exposure of HDF to exogenous forskolin resulted in rapid phosphorylation of CREB at serine 133, consistent with previous results obtained in HaCaT keratinocytes (20). Similarly, the membrane-permeable cAMP analog Bt_2cAMP led to a comparable extent of CREB phosphorylation. Co-incubation with forskolin plus Bt_2cAMP did not have an additive effect on CREB phosphorylation suggesting already maximal activation of cAMP-activated CREB kinases, *e.g.* PKA, by each individual stimulus. The ability of forskolin to activate cAMP-dependent gene transactivation in HDF was verified in experiments using pCRE-luc, a reporter construct consisting of three CREs cloned upstream of the SV40 promoter, driving the expression of the luciferase gene. As shown in Fig. 1*B*, forskolin efficiently transactivated the CRE-dependent construct, 12–16-fold above unstimulated control values (Fig. 1*B*). Together, these results demonstrate the functionality of the cAMP-PKA-CREB cascade in HDF and warrant further investigation into the interference of cAMP-elevating agents with TGF-β-mediated signaling in our experimental system.

Activation of Adenylate Cyclase Attenuates TGF-β-induced Collagen and CTGF Synthesis by HDF in Vitro—Next, we examined the effect of increased cAMP levels on collagen expression and secretion. TGF-β, a prototypical inducer of collagen synthesis, was used in all experiments. HDF were stimulated with forskolin, TGF-β, or both agents for 24 h. The relative mRNA steady-state levels for the α1 and α2 chains of collagen type I (alleles *COL1A1* and *COL1A2*, respectively) were subsequently determined by quantitative real time PCR. TGF-β significantly increased the mRNA levels of collagen type I (α1 and α2) compared with nontreated cells (Fig. 1, *C* and *D*). The observed rate of increase in the amount of these collagens by TGF-β was in accordance with earlier reports (27). Forskolin suppressed the levels of collagen type I α1 as compared with

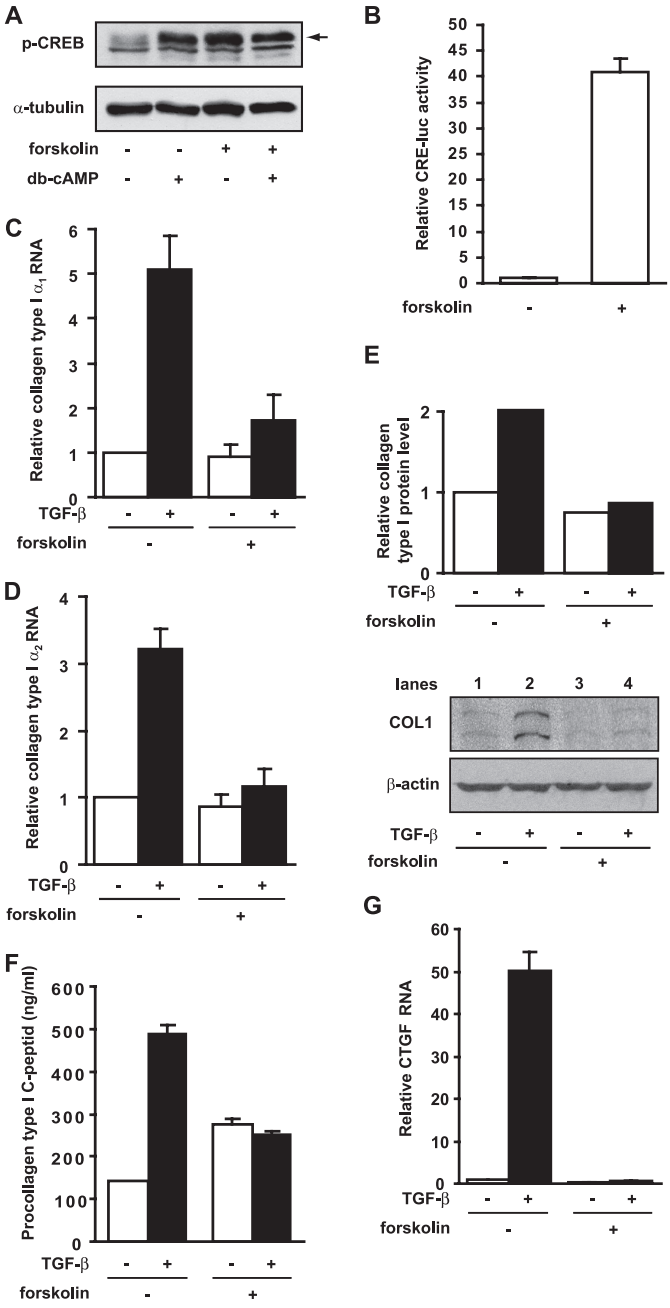

FIGURE 1. **Forskolin elicits a CRE-dependent response in HDF and suppresses collagen synthesis by HDF *in vitro*.** *A,* subconfluent HDF were stimulated with forskolin (20 μM), Bt_2cAMP (*db-cAMP*) (1 mM), forskolin plus Bt_2cAMP or were left untreated (−). After 30 min, cells were lysed and samples processed for Western immunoblotting with specific antibodies for phospho-Ser-133-CREB and α-tubulin. *B,* subconfluent HDF were transfected with pCRE-luc in medium supplemented with 1% FCS. 16 h after transfection, forskolin (20 μM) was added, and incubations were continued for 6 h after which reporter gene activity was determined. *C* and *D,* subconfluent HDF were left untreated or were stimulated with forskolin (20 μM) in the presence (+) or absence (−) of TGF-β (10 ng/ml). Twenty four h later, collagen type I α1 and α2 mRNA levels were analyzed by real time PCR. *E,* confluent HDF were stimulated with TGF-β, forskolin, both substances, or were left untreated for 24 h in a medium containing 1% FCS. Type I collagen expression was examined by Western immunoblotting of whole-cell lysates (100 μg/lane) (*top*). Specificity of the modulation and identical protein loading was confirmed with an anti-β-actin antibody (*lower panel*). Densitometric analysis of the total collagen type I protein expression was performed (*upper panel*). *F,* confluent HDF were stimulated for 48 h with the indicated agents at concentrations described above. Immunoreactive amounts of PICP present in the culture media were determined by ELISA. *G,* after stimulation of HDF with the indicated agents for 24 h, CTGF mRNA levels were analyzed by real time PCR.

cells stimulated with TGF-β alone almost back to basal levels (Fig. 1*C*, $p < 0.01$). Likewise, forskolin repressed TGF-β-induced *COL1A2* expression as compared with cells stimulated with TGF-β alone (Fig. 1*D*, $p < 0.01$). Forskolin alone did not have any significant effect on the relative levels of *COL1A1* and *COL1A2* mRNAs (Fig. 1, *C* and *D*).

To further confirm the modulatory effect of forskolin on TGF-β-induced collagen synthesis, we performed Western immunoblot analysis of whole-cell lysates using an anti-type I collagen antibody. In accordance with the antagonistic effect of forskolin on collagen type I RNA expression, the intracellular amounts of type I collagen production in response to TGF-β were lower in the presence of forskolin, although actin levels remained unchanged throughout the experiments (Fig. 1*E*).

To investigate whether the effect of increased intracellular cAMP levels on collagen synthesis translates into the amount of secreted collagen, we determined the amount of procollagen I C-terminal peptide (PICP) in the culture media of HDF stimulated with forskolin, TGF-β, or both agents. The addition of TGF-β led to a substantial increase of PICP in the culture medium (Fig. 1*F*). In accordance with the modulatory effect of forskolin on TGF-β-induced collagen expression at RNA and the protein level, we found significantly reduced amounts of PICP secreted by HDF (Fig. 1*F*). Unexpectedly, forskolin alone appeared to increase the amount of secreted PICP as compared with untreated controls. This effect may be attributable to an extracellular mechanism in regulation of collagen synthesis, *e.g.* reduced extracellular proteolytic degradation by cAMP-regulated membrane-bound proteinases (28).

Next, we determined the effect of increased cAMP levels on another TGF-β target gene, *CTGF*. Previously, it was reported that *CTGF* is regulated in a Smad-dependent fashion and as a downstream modulator of several profibrotic TGF-β effects (29–32). In HDF, TGF-β stimulation dramatically enhanced mRNA levels of *CTGF*, although a combined incubation with forskolin led to an expression level comparable with untreated HDF (Fig. 1*G*).

Together, these data demonstrate that increased cAMP levels have significant effects on TGF-β-induced type I collagen synthesis. Forskolin acts as a repressor of TGF-β-mediated *COL1A1/2* expression, subsequently leading to decreased intracellular and secreted amounts of collagen type I. This modulatory effect might in part be mediated by CTGF, as CTGF inhibition is reported to suppress excessive collagen deposition in various *in vitro* and *in vivo* models (11, 29, 30, 33).

Activation of Adenylate Cyclase Prevents TGF-β-induced Gene Expression of Proteinase Inhibitors—To further extend the observed antagonistic effect of increased cAMP levels on TGF-β-induced gene regulation, we investigated those encoding the proteinase inhibitors PAI-1 and TIMP1, two well known modulators of ECM deposition (34, 35). Both genes have been shown previously to be regulated in response to TGF-β stringently in a Smad-dependent manner (10, 36–38). As a first approach, HDF were transiently transfected with reporter construct p800-luc, which consists of 800 bp of the human *PAI-1* promoter driving the expression of the luciferase gene (19). As shown in Fig. 2*A*, TGF-β enhanced p800-luc activity 7–9-fold above control levels. Addition of forskolin completely abolished the TGF-β response and also had a slight effect on basal *PAI-1* promoter activity.

To further substantiate the relevance of such findings obtained with the promoter reporter construct in transient cell transfection experiments, we examined whether endogenous *PAI-1* expression followed the same pattern of regulation. The effect of forskolin on TGF-β-induced *PAI-1* gene expression was therefore examined. As shown in Fig. 2*B*, real time PCR of total RNA samples revealed up-regulation of up to 6-fold by TGF-β that was strongly suppressed by forskolin or Bt_2cAMP. Both treatments alone almost completely abolished basal *PAI-1* expression. Glyceraldehyde-3-phosphate dehydrogenase mRNA steady-state levels were unaffected confirming the specificity of *PAI-1* regulation. These suppressive effects on basal *PAI-1* expression may reflect the constant Smad3/4 activation in this cell type even in the absence of exogenous TGF-β. In another set of experiments, PAI-1 production was assessed by Western immunoblotting. HDF were incubated for 48 h with TGF-β in the absence or presence forskolin or Bt_2cAMP. Again, TGF-β strongly elevated PAI-1 production by HDF, but this effect was efficiently blocked by forskolin and Bt_2cAMP. In accordance with the above real time PCR results, cAMP inducers blocked basal PAI-1 protein production, although β-actin levels were not altered by any of the treatments, indicating specificity of basal gene regulation in HDF (Fig. 2*C*).

Similar to *PAI-1*, up-regulation of *TIMP1* by TGF-β was totally suppressed by forskolin or Bt_2cAMP. Of note, neither forskolin nor Bt_2cAMP treatment alone had an impact on basal TIMP1 expression (Fig. 2*D*).

cAMP-elevating Agents Antagonize TGF-β-driven Smad3/4-dependent Gene Expression—To gain insight into the mechanism of the interference between increased cAMP levels and TGF-β-mediated gene expression, we checked if intracellular cAMP levels affect TGF-β-driven transactivation of $(CAGA)_9$-luc, an artificial Smad3/4-specific reporter construct (10). TGF-β efficiently transactivated $(CAGA)_9$-luc in HDF co-transfected (Fig. 3*A*, *left panel*) with empty vector-transfected controls up to 20-fold above control values. A 30-min preincubation of cultured HDF with forskolin resulted in an almost complete inhibition of TGF-β-induced Smad3/4-specific transactivation of $(CAGA)_9$-luc. To prove that inhibition of TGF-β-induced Smad by forskolin is due to specific activation of adenylate cyclase and subsequently increased intracellular cAMP levels, we utilized the membrane-permeable cAMP analog Bt_2cAMP. HDF, transiently transfected with $(CAGA)_9$-luc, were stimulated with Bt_2cAMP in presence or absence of TGF-β. Bt_2cAMP treatment effectively suppressed TGF-β-induced Smad3/4-dependent $(CAGA)_9$-luc gene transactivation, strongly supporting the concept that cAMP plays a pivotal role in the demonstrated TGF-β-opposing phenomenon.

We subsequently tried to determine whether increased cAMP levels are able to directly compete with the downstream effectors of TGF-β-induced gene transcription. For this purpose, an expression vector for Smad3 was co-transfected together with $(CAGA)_9$-luc before stimulation of HDF with TGF-β, in the absence or presence of either forskolin or Bt_2cAMP. As shown in Fig. 3*A* (*right panel*), overexpression of Smad3 resulted already in a significant amplification of

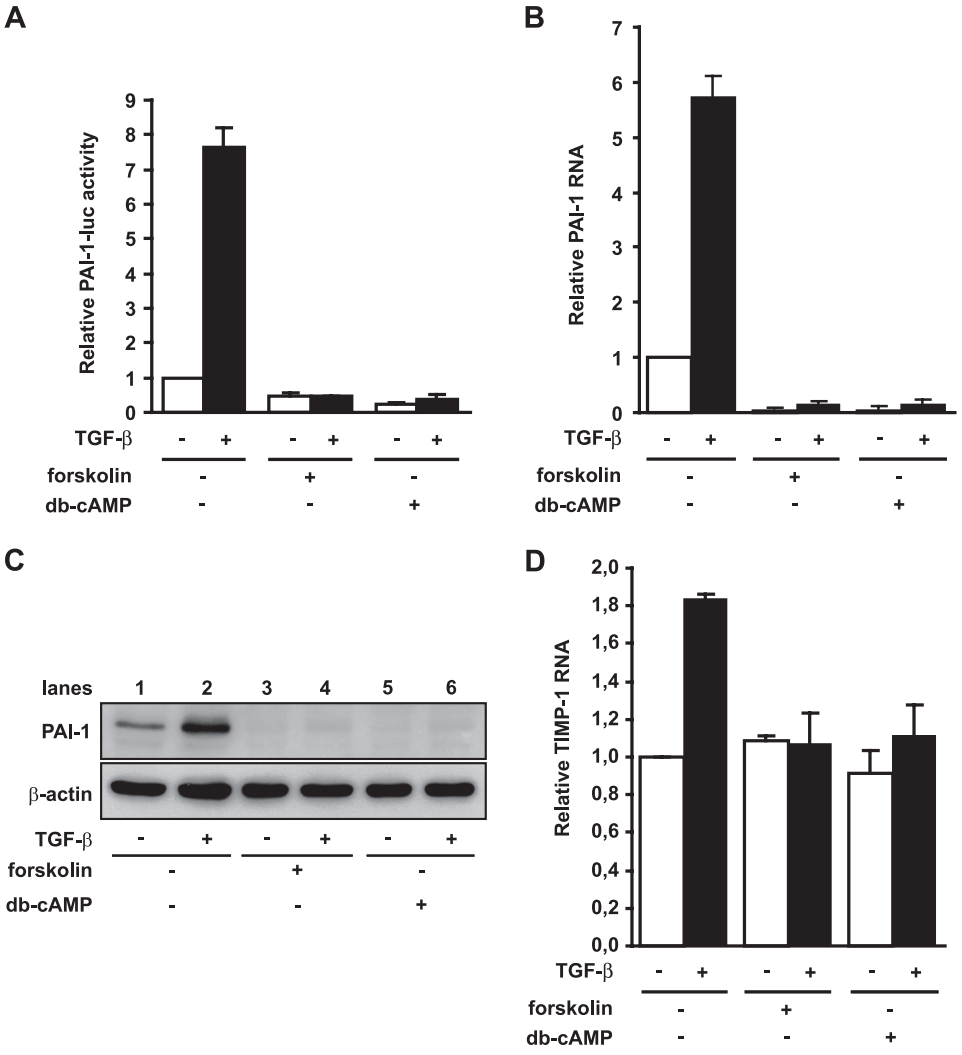

FIGURE 2. **Forskolin and Bt_2cAMP inhibit TGF-β-induced expression of extracellular matrix genes.** *A,* subconfluent HDF were transfected with the *PAI-1* promoter/reporter gene construct p800-luc in a medium supplemented with 1% FCS. 3 h after transfection, forskolin (20 μM) was given in the presence (+) or absence (−) of TGF-β (10 ng/ml). Incubations were continued for 20 h after which the reporter gene activity was determined. Results, presented as relative promoter activity, are means ± S.D. of three experiments each performed on duplicate samples. *B,* subconfluent HDF were stimulated with Bt_2cAMP (*db-cAMP*) (1 mM) or forskolin (20 μM) in the presence (+) or absence (−) of TGF-β (10 ng/ml). 12 h later *PAI-1* mRNA levels were examined by real time PCR. *C,* subconfluent HDF were treated with TGF-β (10 ng/ml) and forskolin (20 μM) or Bt_2cAMP (1 mM) for 24 h in medium containing 1% FCS. After incubation, PAI-1 protein levels were assessed by Western immunoblotting (*top*). Specificity of PAI-1 modulation and identical loading of protein amounts were confirmed using an anti-actin antibody (*bottom*). Results from a representative experiment are shown. *D,* subconfluent HDF were left untreated or treated with forskolin (20 μM) or Bt_2cAMP (1 mM) in the presence (+) or absence (−) of TGF-β (10 ng/ml), and 12 h later *TIMP1* mRNA levels were examined by real time PCR.

$(CAGA)_9$-luc activity as compared with empty vector-transfected controls (*left panel*). Treatment of Smad3-co-transfected HDF with TGF-β led to more than a 2–3-fold increase of CAGA-luc activity (resulting in a up to 60-fold activity) as compared with CMVe-transfected, TGF-β-treated controls. On the contrary, forskolin- or Bt_2cAMP-treated, Smad3-co-transfected HDF exhibited only marginally Smad-dependent gene transactivation upon TGF-β stimulation, and Smad3-induced basal $(CAGA)_9$-luc was almost completely abolished by either agent.

cAMP Does Not Affect Smad Protein Phosphorylation and Nuclear Translocation in Response to TGF-β—To gain more insight into the molecular mechanism underlying the inhibitory activity of the cAMP pathway against TβRI-initiated Smad signaling, we determined the levels of phospho-Smad3 in HDF treated with forskolin or Bt_2cAMP in the presence or absence of TGF-β. Results presented in Fig. 3*B* confirmed the absence of phosphorylated Smad3 in nonstimulated HDF. TGF-β strongly induced phosphorylation of TGF-β receptor-associated Smad3. Co-incubation with neither forskolin nor Bt_2cAMP affected Smad3 phosphorylation in the presence of TGF-β.

Next, we examined whether forskolin or Bt_2cAMP interferes with the translocation of Smad proteins induced by TGF-β. To this purpose, HDF were pretreated or not with forskolin or Bt_2cAMP before TGF-β was added for 30 min. An antibody directed against Smad2/Smad3, the specific substrates for activated TβRI, was used to determine their cellular localization (Fig. 3*C*). Slides were counterstained with 4′,6-diamidino-2-phenylindole to localize cell nuclei precisely. As shown in Fig. 3*C, upper left panel*, a weak and diffuse signal specific for Smad2/3 was present in both the cytoplasm and nuclei in the unstimulated HDF (*left panel*). Co-incubation with neither forskolin nor Bt_2cAMP caused any significant change in the staining pattern. TGF-β induced a rapid and complete nuclear translocation of all Smad2/3-specific immunoreactivity (*right panel*), which was not affected by co-incubation with forskolin or Bt_2cAMP otherwise sufficient to interfere with Smad-dependent transcription (Fig. 3*C*).

Interestingly, in cardiac fibroblasts, cAMP-elevating agents, *i.e.* isoproterenol, blocked profibrotic effects of TGF-β, *i.e.* collagen expression, largely through inhibiting ERK1/2 phosphorylation (39). However, in HDF, neither TGF-β nor increased cAMP levels had any impact on basal ERK1/2 phosphorylation (data not shown).

CBP/p300 Squelching Is Central to the Interference of the cAMP Cascade with Smad Signaling—The role for CBP/p300 as essential co-activators for Smad-driven gene expression has been well documented (21, 40, 41). Competition for CBP/p300 has also been suggested to mediate some examples of signal-induced transcriptional repression (42–44).

To determine whether the cAMP pathway interferes with Smad3-CBP interactions, we used a method based on the mammalian two-hybrid system (Fig. 4*A*). HDF were transfected with

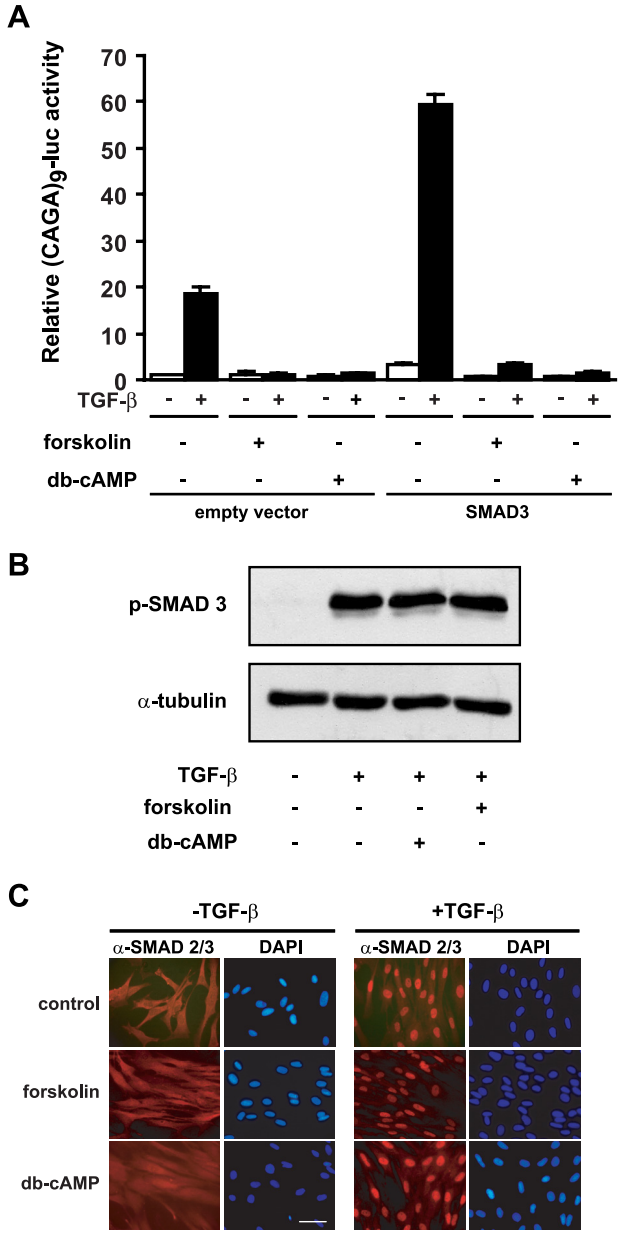

FIGURE 3. **Increased cAMP levels inhibit Smad3/4-dependent transcription without alteration of Smad3 phosphorylation and nuclear translocation in response to TGF-β in HDF.** *A,* subconfluent cells were transfected with a Smad-dependent promoter/reporter construct $(CAGA)_9$-luc, together with expression vectors for Smad3 or the corresponding empty vector in a medium supplemented with 1% FCS. 6 h after transfection, forskolin (20 μM) or Bt_2cAMP (*db-cAMP*) (1 mM) was added in the presence (+) or absence of TGF-β (10 ng/ml). Incubations were continued for 20 h after which the reporter gene activity was determined. Results of a representative experiment performed on duplicate samples are shown as relative luciferase activity. *B,* subconfluent HDF were treated with TGF-β (10 ng/ml) in the presence or absence of forskolin (20 μM) or Bt_2 cAMP (1 mM) left untreated. After 30 min, cells were lysed, and samples were processed for Western immunoblotting with specific antibodies for phospho-Smad3 and α-tubulin. *C,* subconfluent HDF in eight-well tissue chambers were incubated with forskolin (20 μM) or Bt_2cAMP (1 mM) together with TGF-β (10 ng/ml). After 30 min, cells were fixed and double-stained with a Smad2/3 antibody (*red signal*) and with 4′,6-diamidino-2-phenylindole (*DAPI*) to visualize cell nuclei (*blue signal*) followed by fluorescence microscopy (*scale bar,* 25 μm).

a G5E1b-luc reporter construct together with a Gal4 DNA binding domain-Smad3 fusion protein (Gal4-Smad3) expression vector, in the absence or presence of a VP16 activation

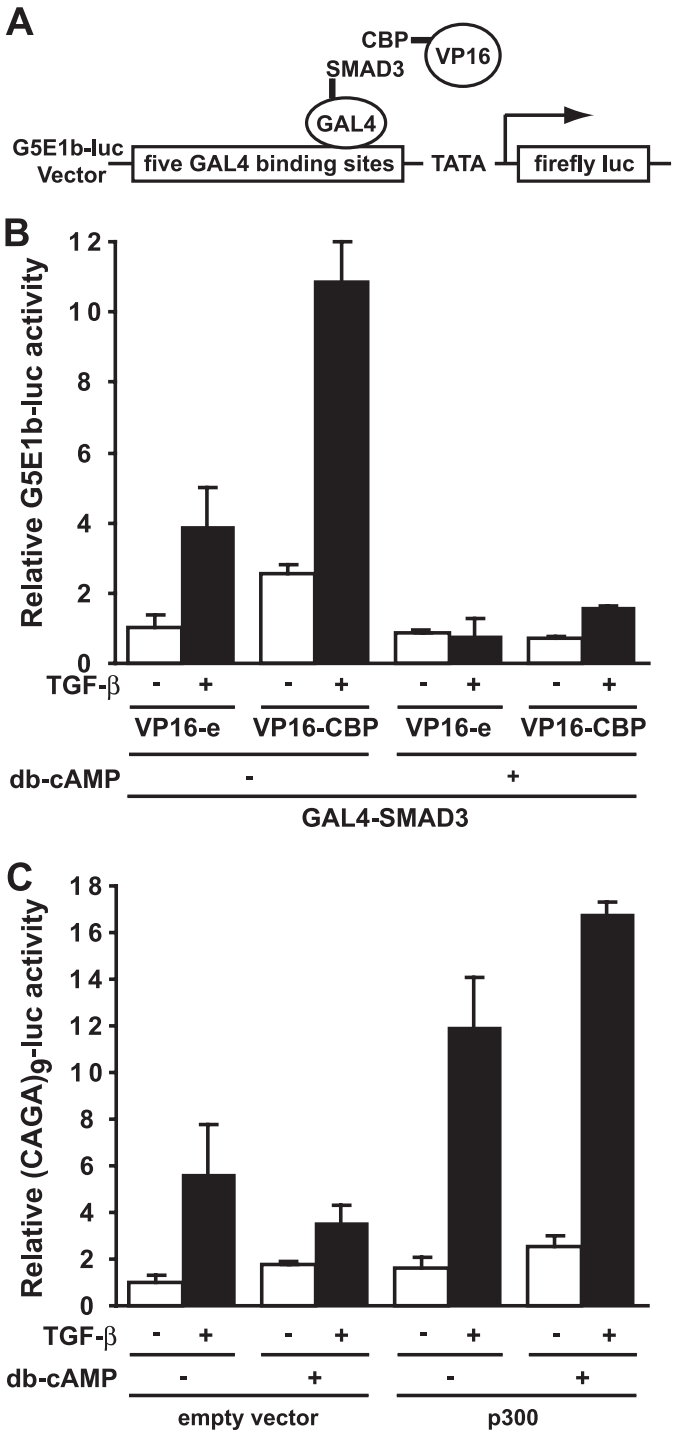

FIGURE 4. **Bt_2cAMP prevents the interaction of Smad3 with its co-activators CBP/p300.** *A,* schematic representation of the mammalian two-hybrid system used to detect protein-protein interactions between Smad3 and CBP. Interaction results in transcription of the firefly luciferase (*luc*) reporter gene. *B,* subconfluent HDF cultures were transfected with G5E1b-luc and Gal4-Smad3 and with VP16-empty or with VP16-CBP. 24 h later, TGF-β (5 ng/ml) was added where indicated, following (+) or not (−) a 30-min preincubation with Bt_2cAMP (*db-cAMP*) (500 μM). G5E1b-luc activity was determined 16 h later. *C,* subconfluent HDF were transfected with $(CAGA)_9$-luc, together with either empty pcDNA or p300 expression vector. 24 h later, Bt_2cAMP (500 μM) was added, and incubations were continued for another 16 h in the absence (−) or presence (+) of TGF-β (5 ng/ml) before reporter gene activity was determined. Results, presented as relative promoter activity, are means ± S.D. of three experiments performed each on duplicate samples.

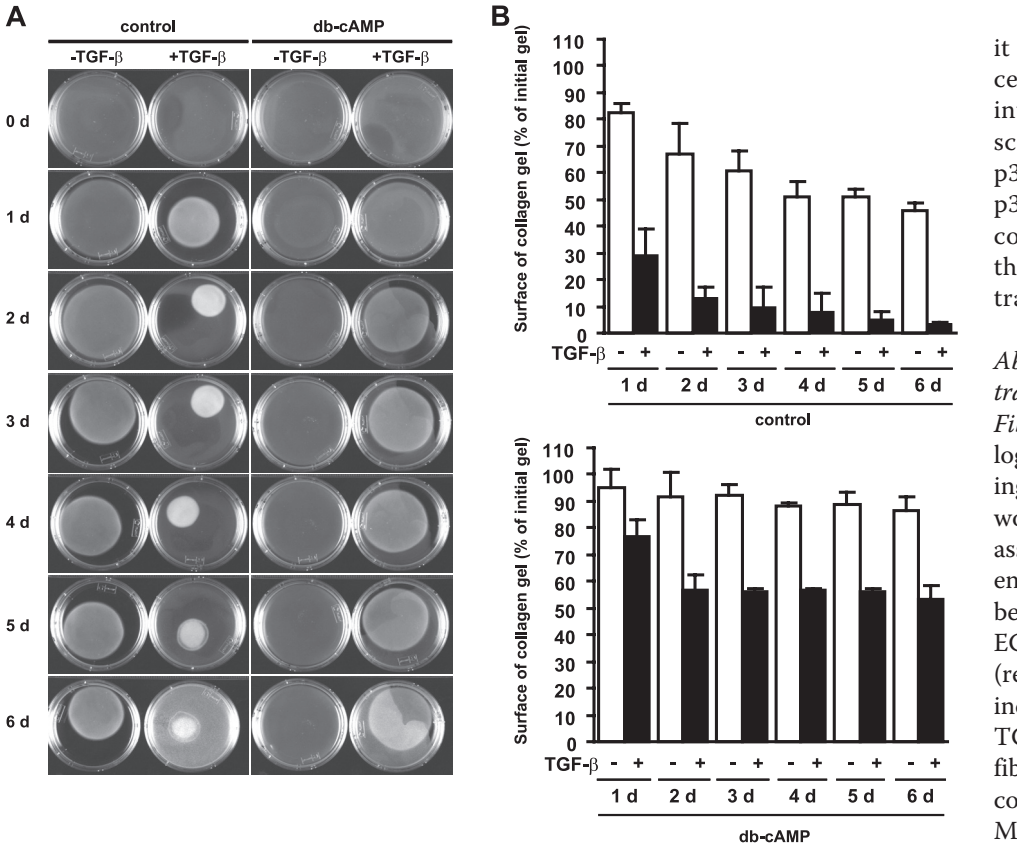

FIGURE 5. **Antagonistic effect of cAMP on the contraction of collagen gels by fibroblasts.** Contraction of free-floating collagen lattices seeded with immortalized murine fibroblasts (NIH3T3) (for details see "Experimental Procedures") was carried out at the time points shown (1–6 days (*d*)). Lattices were treated with Bt_2cAMP (*db-cAMP*) (1 mM) or without in the absence (−) or presence (+) of TGF-β (10 ng/ml). *A,* photographs of a representative experiment. *B,* surface area of collagen gels was calculated at the time points indicated and expressed as a percentage, with the surface area of the noncontracted state serving as 100%. Values represent means ± S.D. of at least three independent experiments.

domain-CBP (VP-CBP) fusion expression vector. As shown in Fig. 4*B*, Gal4-Smad3 transactivated G5E1b-luc in the presence of TGF-β, representative of the transactivation property of phosphorylated Smad3. Co-expression of VP-CBP together with Gal4-Smad3 strongly enhanced luciferase activity, representative of Smad3-CBP interaction. The latter was efficiently abolished by exogenously added Bt_2cAMP, suggesting that activation of the cAMP/CREB pathway affects the association of Smad3 with the transcriptional co-activators CBP/p300.

Because the amount of CBP/p300 is limiting within the cell nucleus (45), formation of CREB-p300 complexes may reduce the amount of co-activators available to Smad3 for optimal transcription. If this scenario is correct, then overexpression of p300 should overcome the inhibitory effect of cAMP on TGF-β/Smad3 activation of the $(CAGA)_9$-luc construct. To test this hypothesis, we measured the effect of p300 overexpression on Bt_2cAMP inhibition of $(CAGA)_9$-luc transactivation by TGF-β. As shown in Fig. 4*C*, p300 overexpression not only prevented but reversed the inhibitory effect of Bt_2cAMP, thereby indicating that CBP/p300 is a critical player in the interference of cAMP with the Smad pathway. It should also be noted that p300 overexpression resulted in increased $(CAGA)_9$-luc activity in response to TGF-β stimulation, a result that is consistent with the concept of limited availability of p300, and confirms the role of p300 as a Smad3 co-activator (21, 40, 41).

From the data presented above, it appears that elevation of intracellular cAMP directly affects the interaction of Smad3 with its transcriptional co-activators CBP and p300. This effect is probably due to p300/CBP squelching from Smad complexes by CREB, resulting in the blockade of Smad-specific transcription.

Synthetic cAMP Significantly Abolishes Smad-dependent Contraction of Collagen Gels by Fibroblasts—To study the physiological relevance of the above findings, we next utilized an *in vitro* wound contraction model. This bioassay utilizes NIH3T3 fibroblasts embedded in type I collagen and has been used as an *in vitro* model for ECM remodeling and cell motility (reviewed in Ref. 46). Recent data indicate that Smad3 is critical in TGF-β-mediated augmentation of fibroblast-mediated collagen gel contraction, whereas ERK and p38 MAPK pathways do not appear to be involved in this process (47, 48). As shown in Fig. 5, *A, left panel,* and *B, upper panel*, NIH3T3 cells in the absence of any stimulus readily contracted the collagen gel within 6 days to ~50% the size as compared with gels without cells. TGF-β drastically accelerated gel contraction. Within 24 h after separation of the gel from the wells, the total area of the free floating, mechanically unloaded gels declined to 30% of the original lattice size, and finally reached less than 10% of the original gel size within 6 days. Co-incubation with Bt_2cAMP or forskolin (data not shown) completely abolished spontaneous contraction of collagen gels by NIH3T3 fibroblasts. Moreover, TGF-β-mediated enhancement of the contractile activity was strongly blocked by the cAMP-inducing agents. These results demonstrate that increased intracellular cAMP levels completely neutralize the capacity of unstimulated or TGF-β-treated fibroblasts to contract collagen gels. Comparable results could be obtained with HDF; however, rapid spontaneous contraction of collagen gels by HDF was, in our hands, much more pronounced than by NIH3T3 fibroblasts (data not shown).

Increased Intracellular cAMP Levels Inhibit Fibroblast Migration in an in Vitro Wound Model—We then investigated the effect of increased cAMP levels on fibroblast motility. In a modified scratch migration assay, HDF migrated into the wound area and completely closed it within 72 h (Fig. 6*A*). On the other hand, in the presence of forskolin, the wound remained open within the recorded time period of 72 h (Fig. 6*A*). Quantification of the wound closure over time revealed a significant inhibitory effect of forskolin on fibroblast motility

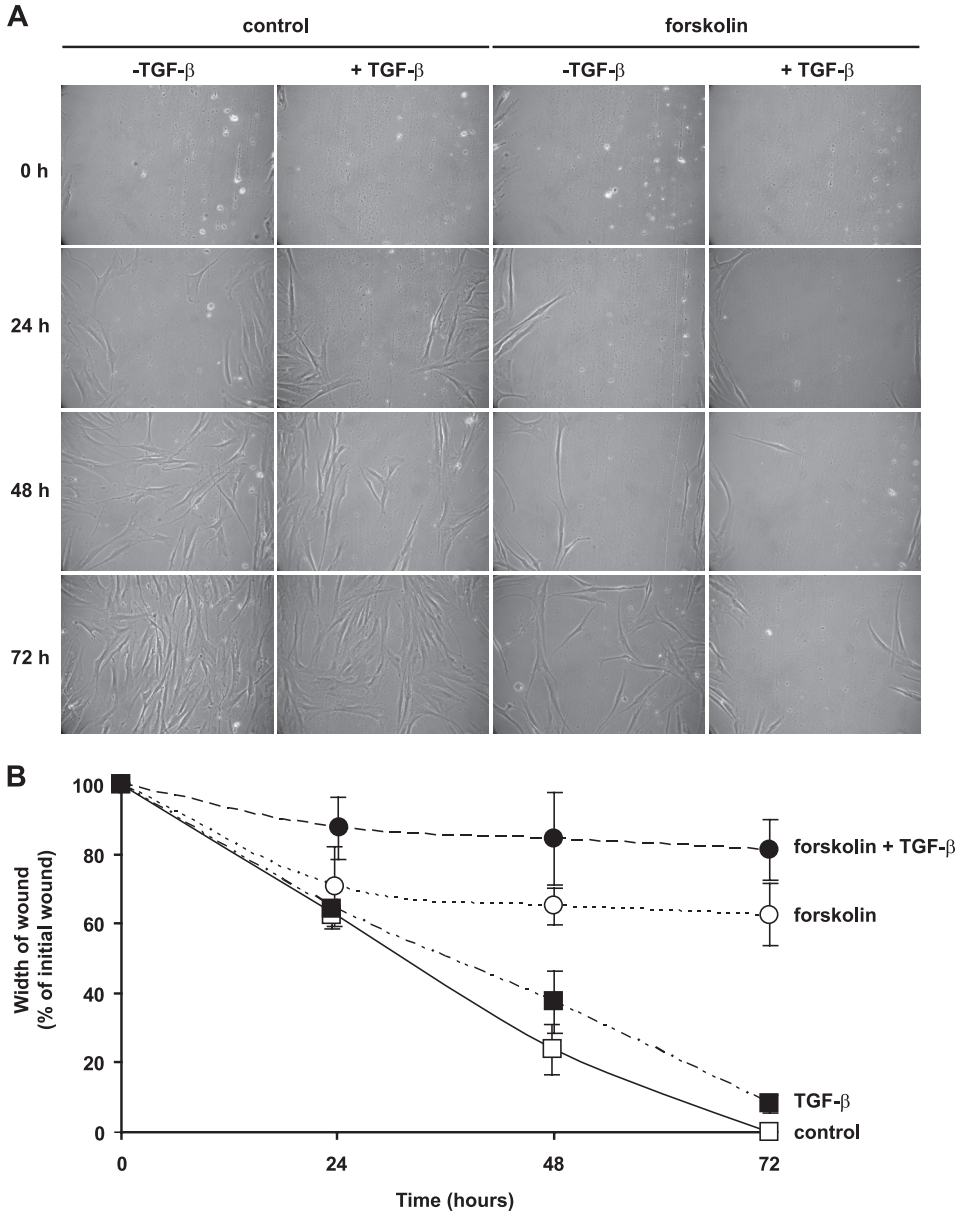

FIGURE 6. **Increased intracellular cAMP levels suppress the migration of fibroblasts.** Confluent HDF cultures were investigated for their potential to migrate into a cell-free scratch region. *A,* after applying an ~0.8-mm scratch with a pipette tip, cell culture medium was replaced with fresh medium containing 10% FCS with or without forskolin (20 μM) in the presence (+) or absence (−) of TGF-β. Migration was monitored by inverted light microscopy. A representative micrograph for each condition is shown, taken immediately, 24, 48, or 72 h after wounding. *B,* graphic representation of the mean of two experiments as indicated. For each sample, the value is corrected against the width of the wound at the start of the experiment.

(Fig. 6*B*). Because TGF-β is a known activator of fibroblast motility (49), we tried to determine whether TGF-β would be able to accelerate fibroblast migration in the absence or presence of forskolin. However, when HDF cells were treated with TGF-β, no significant difference in migration within the wound was observed as compared with untreated cultures (Fig. 6, *A* and *B*). In addition, in TGF-β- and forskolin-treated fibroblasts, no statistically significant difference in migration within the wound area could be detected as compared with Bt_2cAMP-treated cultures alone (Fig. 6, *A* and *B*), indicating that TGF-β cannot overcome the impairment in motility induced by increased intracellular cAMP levels.

cAMP Does Not Antagonize but Synergizes with TGF-β to Enhance Hyaluronan Synthesis—To investigate the specificity of the antagonistic effect of increased cAMP levels on TGF-β-mediated effects in HDF, we finally investigated the impact of Bt_2cAMP on TGF-β-mediated synthesis of hyaluronan (HA), another prominent constituent of the ECM. HA is a nonsulfated acidic carbohydrate consisting of repeating disaccharide units. It is synthesized by three HA synthase isoforms (HAS1–3), located at the inner surface of the cell membrane. TGF-β is known as a potent inducer of HA synthesis in synovial and lung fibroblast (50, 51). For this purpose, HDF were stimulated with TGF-β, Bt_2cAMP, TGF-β plus Bt_2cAMP, or were left untreated. As shown in Fig. 7*A*, TGF-β alone did not increase HAS2 mRNA levels, although treatment of HDF with Bt_2cAMP resulted in a 3-fold increase of HAS2 mRNA levels as shown by real time PCR. However, the effect of Bt_2cAMP on the relative levels of HAS2 mRNA was significantly enhanced when TGF-β and Bt_2cAMP were co-incubated (Fig. 7*A*). To confirm the synergistic or additive effects of TGF-β and cAMP, we measured HA synthesis. HDF were incubated for 48 h as outlined above, and HA in supernatants was subsequently determined by ELISA. TGF-β and Bt_2cAMP alone had weak but reproducible up-regulating effects on HA synthesis. However, TGF-β and Bt_2cAMP acted synergistically on secreted HA levels compared with cells treated with each stimulus alone (Fig. 7*B*).

Comparative Regulatory Sequence Analysis of cAMP Differentially Regulated ECM Genes—We hypothesized that ECM genes exhibiting a common regulatory behavior upon cAMP stimulation, *i.e.* up-regulation, may also share common regulatory mechanisms such as the presence or absence of certain transcription factor-binding sites in their promoter regions. To identify these possible cAMP-responsive elements presumably over-represented in the *HAS2* gene, we utilized the web-based Genomatix bioinformatics software (25). As expected, Smad-binding elements were identified in all ECM genes (*PAI-1*, *COL1A1*, *COL1A2*, *CTGF*, *TIMP1*, and *HAS2*) that were evaluated ($p < 0.0001$). The MatInspector tool detected three CREB DNA-binding sites along with seven puta-

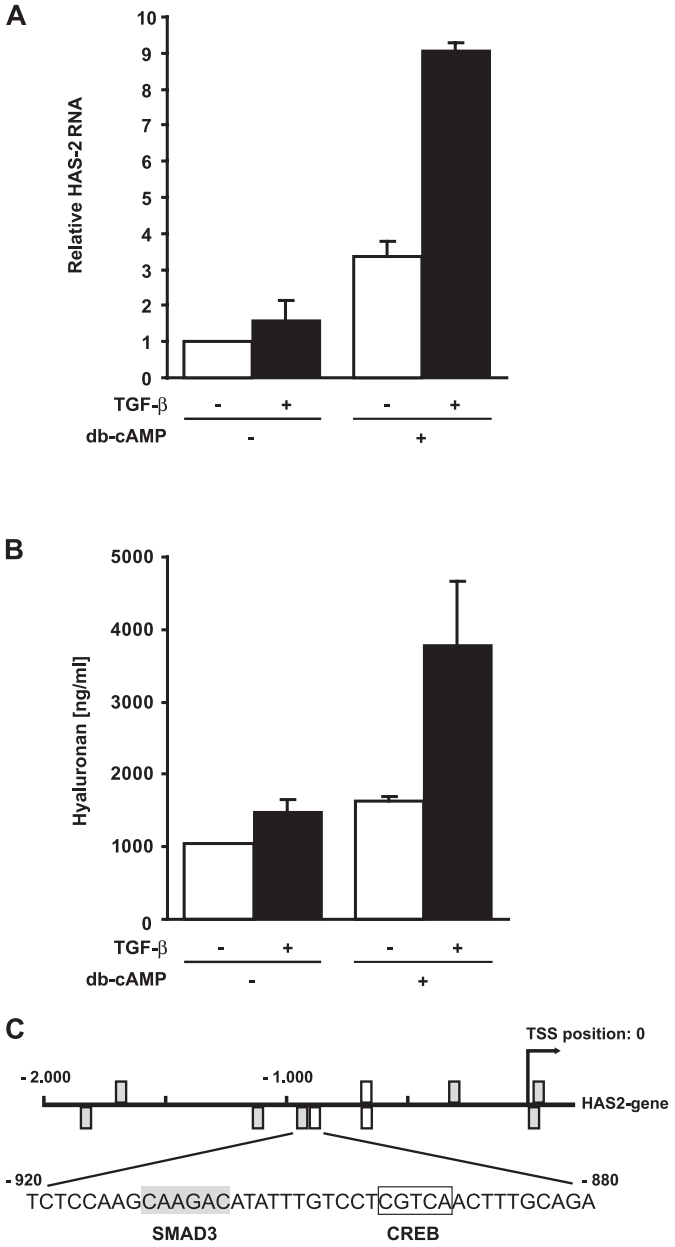

FIGURE 7. **TGF-β potentiates cAMP-mediated up-regulation of *HAS2* mRNA and HA.** *A,* subconfluent HDF were stimulated with Bt_2cAMP (*db-cAMP*) (1 mM) in the presence (+) or absence (−) of TGF-β (10 ng/ml), in a medium supplemented with 1% FCS. 24 h later, HAS2 mRNA levels were detected by real time PCR. One representative experiment out of three is shown. *B,* subconfluent HDF were treated with TGF-β (10 ng/ml) and Bt_2cAMP (1 mM) for 48 h in medium containing 1% FCS. After incubations, total HA levels were detected by a commercially available ELISA. Values represent means ± S.D. of at least three independent experiments. *C,* computational analysis of the regulatory elements of HAS2. CREB- and Smad3-binding sites were identified by scanning the 5′ promoter region of the *HAS2* gene with MatInspector. Each block represents a match; *white blocks* are CREB sites; *gray blocks* are Smad3 sites. The *number* on the axis refer to bases 5′ upstream from transcription start sites.

tive Smad3-binding sites in the *HAS2* promoter only (Fig. 7*C*). One region of potential interest in the *HAS2* promoter, which contains a Smad3-binding site and a CREB site within 10 bp of each other, is also highlighted in Fig. 7*C*. Noteworthy, functional CREB-binding sites were recently characterized within the human *HAS2* gene (52).

In summary, these data demonstrate that cAMP differentially regulates important components of the ECM. Although cAMP most likely via activated CREB antagonize the anabolic effects of TGF-β on ECM deposition and wound contraction, TGF-β and cAMP have additive effects on *HAS2* expression and HA secretion presumably by a promoter-mediated mechanism.

DISCUSSION

In this study, we have evaluated the *in vitro* effects of increased intracellular cAMP levels on various key effector functions of fibroblasts. Our data demonstrate that elevation of intracellular cAMP by artificial stimulators such as the fungal drug forskolin or Bt_2cAMP has multidirectional functional consequences, either stimulatory or inhibitory, on Smad-dependent genes, on collagen synthesis and contraction, production of HA, and fibroblast migration. In particular, our data provide profound evidence for a functional interaction between the cAMP/CREB and TGF-β signaling pathway in HDF.

The biological relevance of our findings is supported by the fact that several physiological mediators and hormones, such as the pro-opiomelanocortin-derived peptide α-melanocyte-stimulating hormone (α-MSH), catecholamines, or prostaglandins, can bind to fibroblasts via specific receptors and subsequently activate adenylate cyclase. For example, we showed that human dermal fibroblastic cells have the full enzyme machinery and capacity to generate pro-opiomelanocortin peptides (53, 54). These cells also express the melanocortin-1 receptor, a small G-protein-coupled receptor with seven transmembrane domains, whose engagement with α-MSH leads to increased cAMP levels in human dermal fibroblasts (26, 54). Treatment of the cells with α-MSH significantly attenuated TGF-β-mediated collagen synthesis *in vitro* and as well as in a mouse model of dermal fibrosis induced by repetitive injection of high amounts of TGF-β (26). Thus, the antagonistic effect of α-MSH on TGF-β-mediated collagen synthesis is in accordance with the herein observed suppressive action of forskolin on TGF-β-induced collagen type I protein expression and PICP secretion. However, in HDF α-MSH did not have any robust effect on TGF-β-induced collagen transcription and acted at the post-transcriptional level. The reason for these distinct differences in the effect of the natural cAMP inducer α-MSH and the synthetic drug forskolin with regard to suppression of collagen synthesis remains unknown but may be related to the relative levels of cAMP induced by each agent. Moreover, α-MSH has been shown to affect simultaneously a diversity of signal transduction pathways (55), which may be differentially regulated by forskolin. Interestingly, in human embryo lung fibroblasts (IMR90) expressing the EP2 receptor, prostaglandin E_2 as well as the synthetic analog 11-deoxyprostaglandin E_1 also had profound inhibitory actions on basal and TGF-β-induced collagen mRNA levels (56).

The reduction in the relative RNA levels of collagen type I after co-treatment with TGF-β and natural or artificial intracellular cAMP inducers suggested to us interference with the classical signal transduction pathway of TGF-β as the potential molecular mechanism of the observed cAMP effect. In fact, our reporter-promoter assays employing the $(CAGA)_9$-luc construct revealed significantly reduced transactivation by Smad3/

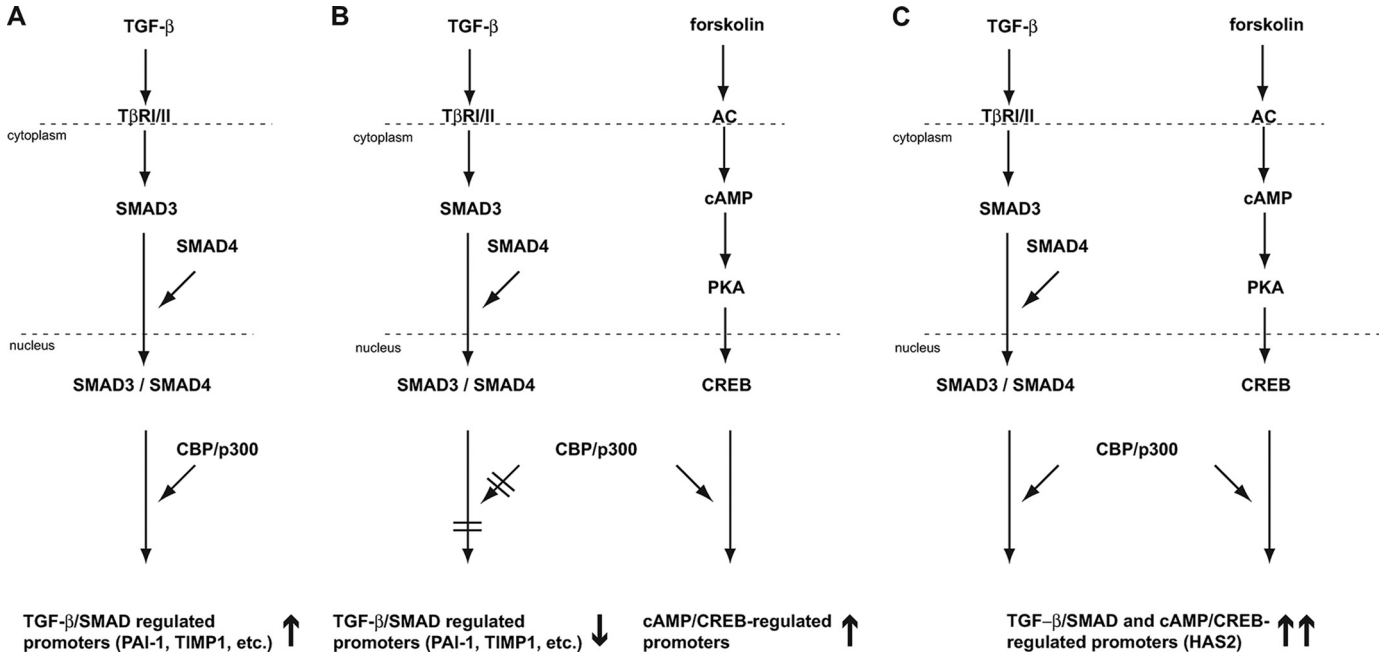

FIGURE 8. **Transcriptional activation and repression of ECM genes.** *A,* Smad-dependent transcriptional activation. *B,* cAMP-induced CREB activation abrogates Smad-dependent gene expression by squelching the CBP/p300 transcriptional co-activator. *C,* integration of TGF-β and cAMP-induced activation of *HAS2* gene on the promoter level by shared transcription factors, *i.e.* CREB and Smad3 and common cofactors like CBP/p300 (for further details see text).

4 after co-incubation with Bt_2cAMP and TGF-β. The negative impact of increased intracellular levels of cAMP on Smad-dependent gene expression is further supported by the robust effect on PAI-1, a *bona fide* Smad3/4-dependent gene. Both forskolin and Bt_2cAMP abrogated RNA and protein expression of PAI-1 and *PAI-1* promoter activity induced by TGF-β. The impact of forskolin on the basal levels of PAI-1 synthesis does not rule out the Smad3/4 specificity of this effect, but rather it may reflect a constant Smad3/4 activation in this cell type even in the absence of exogenous TGF-β (57, 58).

Our results provide definitive evidence that cAMP-elevating agents interfere with TGF-β-specific Smad3/4-dependent gene expression via reduction of Smad3-CBP/p300 interactions and potential sequestration of the transcriptional co-activators CBP/p300 by phosphorylated CREB. Recently, it has been shown that not only prevention of CBP/p300 recruitment but also p300-mediated histone H4 hyperacetylation on TGF-β-responsive promoters, *e.g. COL1A2*, were responsible for such a mechanism (43). Although it is plausible that the suppressive effect of artificial or natural cAMP inducers on TGF-β-mediated collagen synthesis is mediated via squelching of the above transcription factors, it should be noted that transcriptional regulation of *COL1A1*, *COL1A2,* and *COL3A1 sensu strictu* is in part independent of Smad proteins as shown by SP1 antisense approaches and mutational analysis of Sp1 sites (GC box) within the promoter regions of such genes (59, 60). Therefore, the molecular mechanism by which elevated cAMP levels suppress TGF-β-induced collagen synthesis still requires further elucidation. One potential alternative mechanism may reside in transcriptional repression of *CTGF*. Knockdown of *CTGF* abolishes collagen deposition in various *in vitro* and *in vivo* models (11, 29, 30, 33). We showed that TGF-β-stimulated *CTGF* expression is completely abolished by incubation with forskolin. In turn, cAMP-mediated low CTGF levels may block collagen type I expression in HDF. Therefore, the modulatory effects on collagen expression might in part be mediated by CTGF (30, 32).

Our bioassays evaluating gel contraction and fibroblast migration as *in vitro* models for wound closure could further substantiate the functional interference between the TGF-β and the cAMP-CREB pathway. In both assays, Bt_2cAMP robustly blocked TGF-β-induced collagen gel contraction and cell migration. Previously, it has been shown that collagen gel contraction in Smad3 knock-out mice fibroblasts is not affected by TGF-β stimulation (47). Moreover, in HDF-overexpressing Smad3, collagen contraction induced by TGF-β is enhanced, whereas Smad7 overexpression leads to attenuation of TGF-β-induced collagen gel contraction (48, 61). These findings collectively suggest that increased intracellular cAMP levels, apparently by squelching transcription factors of the CBP/p300 family, interfere with Smad-dependent collagen gel induced by TGF-β. On the other hand, it is worth mentioning that increased intracellular cAMP *per se* may affect contraction of collagen as shown by studies with β-adrenoreceptor agonists and antagonists on HDF (62). Accordingly, isoproterenol delayed gel contraction of collagen, and this effect was neutralized by β-adrenoreceptor-specific pharmacological blockade, indicating that the β-adrenoreceptor alone mediates the delay. With regard to the observed suppression of TGF-β-induced migration of HDF cells by Bt_2cAMP, the mechanism by which increased cAMP levels affect this process remains unknown. Several studies suggested a link between cAMP-dependent PKA activation and cellular migration (63–65). Moreover, the effects of cAMP-dependent PKA activation on migration appear to be cell type-specific. Whereas in the majority of cell types PKA activation inhibits cell migration, PKA activation

accelerates the migration of bronchial epithelial cells during wound repair by reducing the levels of active Rho and the formation of focal adhesion (66). On the other hand, it was recently reported that even in fibroblastic cells β-adrenoreceptor-mediated signaling had an Src-dependent promigratory effect (62). This is in contrast to our results in which we found a strong inhibitory effect of Bt_2cAMP on HDF cell migration. Another possibility explaining the different effects of natural and artificial cAMP inducers might be that low levels of increased PKA activity are stimulatory for migration, although higher levels are inhibitory (67, 68). This hypothesis is consistent with findings that dominant negative PKA-expressing cells show reduced stimulation of migration in response to epidermal growth factor/platelet-derived growth factor or serum (69). Indeed, very recent findings revealed that elevated cAMP activates cdc42 via p21-activated kinases in a PKA-dependent manner (70, 71); activated cdc42, a GTPase similar to Rac, is believed to play an important role in regulating actin dynamics and cell adhesion during migration (72).

Finally, it was of interest to investigate if the so-far observed consequences of increased intracellular cAMP levels induced by artificial stimulators would globally act in an antagonistic manner toward TGF-β-mediated effects. As exemplified by analysis of HAS2 mRNA expression and HA protein levels, this was clearly not the case. Bt_2cAMP synergistically enhanced expression of both *HAS2* mRNA and HA protein when co-incubated with TGF-β. Although it is well established that artificial cAMP stimulators can stimulate HA synthesis in various cell types (73–75), we are unaware of any studies addressing the combinatory effect of these agents with TGF-β. Computational analysis of the regulatory elements of *HAS2* identified three CREB- and seven Smad-binding sites within the 5′ promoter region. These data suggest that CREB cooperates with TGF-β-induced downstream signals, *i.e.* Smad3/4 complexes, on the transcriptional level in promoters with cAMP- and TGF-β-response elements. As it has been shown that Smad and CREB do not interact in a direct way (20, 76), CBP/p300 may be the co-activator that mediates the synergy between CREB and Smad3. Such functional cooperation between Smad and CREB family members has been shown for the TGF-β-inducible germ line Igα constant region gene (76). Moreover, this hypothesis is consistent with the fact that cooperative association between CREB- and bone morphogenetic protein-regulated Smads, *i.e.* Smad1/5, has been shown for the *Smad6* promoter containing an 11-bp Smad binding region and an adjacent putative CRE site (77).

Fig. 8 is a diagram illustrating the findings reported in this study. Accordingly, TGF-β- and cAMP-inducing agents, *e.g.* hormones, cooperatively regulate ECM genes and functions. Although the majority of the investigated ECM genes are negatively regulated by the activated cAMP/CREB pathway, it seems that some TGF-β-responsive genes that contain additional CRE elements within their 5′-regulatory region, like *HAS2*, are synergistically activated in a promoter-specific manner. Further studies of the effects of CBP/p300 and other transcription co-activators on the synergistic Smad- and CREB-dependent transcription from the *HAS2* promoter should contribute to our understanding of the complex mechanism of transcriptional regulation by increased cAMP levels and TGF-β.

REFERENCES

1. Brennan, M., Bhatti, H., Nerusu, K. C., Bhagavathula, N., Kang, S., Fisher, G. J., Varani, J., and Voorhees, J. J. (2003) *Photochem. Photobiol.* **78,** 43–48
2. Quan, T., He, T., Kang, S., Voorhees, J. J., and Fisher, G. J. (2004) *Am. J. Pathol.* **165,** 741–751
3. Uitto, J., and Kouba, D. (2000) *J. Dermatol. Sci.* **24,** S60–S69
4. Kokot, A., Sindrilaru, A., Schiller, M., Sunderkötter, C., Kerkhoff, C., Eckes, B., Scharffetter-Kochanek, K., Luger, T. A., and Böhm, M. (2009) *Arthritis Rheum.* **60,** 592–603
5. Schiller, M., Javelaud, D., and Mauviel, A. (2004) *J. Dermatol. Sci.* **35,** 83–92
6. Verrecchia, F., and Mauviel, A. (2002) *Curr. Rheumatol. Rep.* **4,** 143–149
7. Attisano, L., and Wrana, J. L. (2002) *Science* **296,** 1646–1647
8. Massagué, J. (2000) *Nat. Rev. Mol. Cell Biol.* **1,** 169–178
9. Verrecchia, F., and Mauviel, A. (2002) *J. Invest. Dermatol.* **118,** 211–215
10. Dennler, S., Itoh, S., Vivien, D., ten Dijke, P., Huet, S., and Gauthier, J. M. (1998) *EMBO J.* **17,** 3091–3100
11. Holmes, A., Abraham, D. J., Sa, S., Shiwen, X., Black, C. M., and Leask, A. (2001) *J. Biol. Chem.* **276,** 10594–10601
12. Lai, C. F., Feng, X., Nishimura, R., Teitelbaum, S. L., Avioli, L. V., Ross, F. P., and Cheng, S. L. (2000) *J. Biol. Chem.* **275,** 36400–36406
13. Montminy, M. (1997) *Annu. Rev. Biochem.* **66,** 807–822
14. Sassone-Corsi, P. (1998) *Int. J. Biochem. Cell Biol.* **30,** 27–38
15. Chrivia, J. C., Kwok, R. P., Lamb, N., Hagiwara, M., Montminy, M. R., and Goodman, R. H. (1993) *Nature* **365,** 855–859
16. Kwok, R. P., Lundblad, J. R., Chrivia, J. C., Richards, J. P., Bächinger, H. P., Brennan, R. G., Roberts, S. G., Green, M. R., and Goodman, R. H. (1994) *Nature* **370,** 223–226
17. Mayr, B., and Montminy, M. (2001) *Nat. Rev. Mol. Cell Biol.* **2,** 599–609
18. Vindevoghel, L., Lechleider, R. J., Kon, A., de Caestecker, M. P., Uitto, J., Roberts, A. B., and Mauviel, A. (1998) *Proc. Natl. Acad. Sci. U.S.A.* **95,** 14769–14774
19. Keeton, M. R., Curriden, S. A., van Zonneveld, A. J., and Loskutoff, D. J. (1991) *J. Biol. Chem.* **266,** 23048–23052
20. Schiller, M., Verrecchia, F., and Mauviel, A. (2003) *Oncogene* **22,** 8881–8890
21. Dennler, S., Pendaries, V., Tacheau, C., Costas, M. A., Mauviel, A., and Verrecchia, F. (2005) *Oncogene* **24,** 1936–1945
22. Atfi, A., Buisine, M., Mazars, A., and Gespach, C. (1997) *J. Biol. Chem.* **272,** 24731–24734
23. Livak, K. J., and Schmittgen, T. D. (2001) *Methods* **25,** 402–408
24. Cha, D., O'Brien, P., O'Toole, E. A., Woodley, D. T., and Hudson, L. G. (1996) *J. Invest. Dermatol.* **106,** 590–597
25. Cartharius, K., Frech, K., Grote, K., Klocke, B., Haltmeier, M., Klingenhoff, A., Frisch, M., Bayerlein, M., and Werner, T. (2005) *Bioinformatics* **21,** 2933–2942
26. Böhm, M., Raghunath, M., Sunderkötter, C., Schiller, M., Ständer, S., Brzoska, T., Cauvet, T., Schiöth, H. B., Schwarz, T., and Luger, T. A. (2004) *J. Biol. Chem.* **279,** 6959–6966
27. Raghow, R., Postlethwaite, A. E., Keski-Oja, J., Moses, H. L., and Kang, A. H. (1987) *J. Clin. Invest.* **79,** 1285–1288
28. Sawaji, Y., Sato, T., Seiki, M., and Ito, A. (2000) *Clin. Exp. Metastasis* **18,** 131–138
29. Shi-Wen, X., Leask, A., and Abraham, D. (2008) *Cytokine Growth Factor Rev.* **19,** 133–144
30. Leask, A., Holmes, A., and Abraham, D. J. (2002) *Curr. Rheumatol. Rep.* **4,** 136–142
31. Arnott, J. A., Zhang, X., Sanjay, A., Owen, T. A., Smock, S. L., Rehman, S., DeLong, W. G., Safadi, F. F., and Popoff, S. N. (2008) *Bone* **42,** 871–885
32. Leask, A., Holmes, A., Black, C. M., and Abraham, D. J. (2003) *J. Biol. Chem.* **278,** 13008–13015
33. Uchio, K., Graham, M., Dean, N. M., Rosenbaum, J., and Desmoulière, A. (2004) *Wound Repair Regen.* **12,** 60–66
34. Akool, el-S, Doller, A., Müller, R., Gutwein, P., Xin, C., Huwiler, A.,

Pfeilschifter, J., and Eberhardt, W. (2005) *J. Biol. Chem.* **280,** 39403–39416
35. Kolb, M., Margetts, P. J., Sime, P. J., and Gauldie, J. (2001) *Am. J. Physiol. Lung Cell Mol. Physiol.* **280,** L1327–L1334
36. Zhou, X., Hu, H., Huynh, M. L., Kotaru, C., Balzar, S., Trudeau, J. B., and Wenzel, S. E. (2007) *J. Allergy Clin. Immunol.* **119,** 1388–1397
37. Bonniaud, P., Kolb, M., Galt, T., Robertson, J., Robbins, C., Stampfli, M., Lavery, C., Margetts, P. J., Roberts, A. B., and Gauldie, J. (2004) *J. Immunol.* **173,** 2099–2108
38. Vindevoghel, L., Kon, A., Lechleider, R. J., Uitto, J., Roberts, A. B., and Mauviel, A. (1998) *J. Biol. Chem.* **273,** 13053–13057
39. Liu, X., Sun, S. Q., Hassid, A., and Ostrom, R. S. (2006) *Mol. Pharmacol.* **70,** 1992–2003
40. Janknecht, R., Wells, N. J., and Hunter, T. (1998) *Genes Dev.* **12,** 2114–2119
41. Feng, X. H., Zhang, Y., Wu, R. Y., and Derynck, R. (1998) *Genes Dev.* **12,** 2153–2163
42. Ghosh, A. K., Yuan, W., Mori, Y., Chen, Sj., and Varga, J. (2001) *J. Biol. Chem.* **276,** 11041–11048
43. Ghosh, A. K., Bhattacharyya, S., Wei, J., Kim, S., Barak, Y., Mori, Y., and Varga, J. (2009) *FASEB J.* **23,** 2968–2977
44. Verrecchia, F., Pessah, M., Atfi, A., and Mauviel, A. (2000) *J. Biol. Chem.* **275,** 30226–30231
45. Hottiger, M. O., Felzien, L. K., and Nabel, G. J. (1998) *EMBO J.* **17,** 3124–3134
46. Grinnell, F. (1994) *J. Cell Biol.* **124,** 401–404
47. Liu, X., Wen, F. Q., Kobayashi, T., Abe, S., Fang, Q., Piek, E., Bottinger, E. P., Roberts, A. B., and Rennard, S. I. (2003) *Cell Motil. Cytoskeleton* **54,** 248–253
48. Sumiyoshi, K., Nakao, A., Setoguchi, Y., Okumura, K., Tsuboi, R., and Ogawa, H. (2003) *Br. J. Dermatol.* **149,** 464–470
49. Postlethwaite, A. E., Keski-Oja, J., Moses, H. L., and Kang, A. H. (1987) *J. Exp. Med.* **165,** 251–256
50. Westergren-Thorsson, G., Särnstrand, B., Fransson, L. A., and Malmström, A. (1990) *Exp. Cell Res.* **186,** 192–195
51. Tanimoto, K., Suzuki, A., Ohno, S., Honda, K., Tanaka, N., Doi, T., Yoneno, K., Ohno-Nakahara, M., Nakatani, Y., Ueki, M., and Tanne, K. (2004) *J. Dent. Res.* **83,** 40–44
52. Makkonen, K. M., Pasonen-Seppänen, S., Törrönen, K., Tammi, M. I., and Carlberg, C. (2009) *J. Biol. Chem.* **284,** 18270–18281
53. Schiller, M., Raghunath, M., Kubitscheck, U., Scholzen, T. E., Fisbeck, T., Metze, D., Luger, T. A., and Böhm, M. (2001) *J. Invest. Dermatol.* **117,** 227–235
54. Böhm, M., Eickelmann, M., Li, Z., Schneider, S. W., Oji, V., Diederichs, S., Barsh, G. S., Vogt, A., Stieler, K., Blume-Peytavi, U., and Luger, T. A. (2005) *Endocrinology* **146,** 4635–4646
55. Böhm, M., Luger, T. A., Tobin, D. J., and García-Borrón, J. C. (2006) *J. Invest. Dermatol.* **126,** 1966–1975
56. Choung, J., Taylor, L., Thomas, K., Zhou, X., Kagan, H., Yang, X., and Polgar, P. (1998) *J. Cell. Biochem.* **71,** 254–263
57. Schmierer, B., Tournier, A. L., Bates, P. A., and Hill, C. S. (2008) *Proc. Natl. Acad. Sci. U.S.A.* **105,** 6608–6613
58. Schmierer, B., and Hill, C. S. (2005) *Mol. Cell. Biol.* **25,** 9845–9858
59. Verrecchia, F., Rossert, J., and Mauviel, A. (2001) *J. Invest. Dermatol.* **116,** 755–763
60. Poncelet, A. C., and Schnaper, H. W. (2001) *J. Biol. Chem.* **276,** 6983–6992
61. Kopp, J., Preis, E., Said, H., Hafemann, B., Wickert, L., Gressner, A. M., Pallua, N., and Dooley, S. (2005) *J. Biol. Chem.* **280,** 21570–21576
62. Pullar, C. E., and Isseroff, R. R. (2005) *Wound. Repair Regen.* **13,** 405–411
63. Itoh, H., Yamamura, S., Ware, J. A., Zhuang, S., Mii, S., Liu, B., and Kent, K. C. (2001) *Am. J. Physiol. Heart Circ. Physiol.* **281,** H359–H370
64. Kohyama, T., Ertl, R. F., Valenti, V., Spurzem, J., Kawamoto, M., Nakamura, Y., Veys, T., Allegra, L., Romberger, D., and Rennard, S. I. (2001) *Am. J. Physiol. Lung Cell Mol. Physiol.* **281,** L1257–L1263
65. Mukai, M., Nakamura, H., Tatsuta, M., Iwasaki, T., Togawa, A., Imamura, F., and Akedo, H. (2000) *FEBS Lett.* **484,** 69–73
66. Spurzem, J. R., Gupta, J., Veys, T., Kneifl, K. R., Rennard, S. I., and Wyatt, T. A. (2002) *Am. J. Physiol. Lung Cell Mol. Physiol.* **282,** L1108–L1116
67. Elferink, J. G., and VanUffelen, B. E. (1996) *Gen. Pharmacol.* **27,** 387–393
68. Iwasaki, T., Chen, J. D., Kim, J. P., Wynn, K. C., and Woodley, D. T. (1994) *J. Invest. Dermatol.* **102,** 891–897
69. Edin, M. L., Howe, A. K., and Juliano, R. L. (2001) *Exp. Cell Res.* **270,** 214–222
70. Howe, A. K. (2004) *Biochim. Biophys. Acta* **1692,** 159–174
71. Feoktistov, I., Goldstein, A. E., and Biaggioni, I. (2000) *Mol. Pharmacol.* **58,** 903–910
72. Raftopoulou, M., and Hall, A. (2004) *Dev. Biol.* **265,** 23–32
73. Honda, A., Sekiguchi, Y., and Mori, Y. (1993) *Biochem. J.* **292,** 497–502
74. Imai, Y., Ibaraki, K., Odajima, R., and Shishiba, Y. (1994) *Endocr. J.* **41,** 645–654
75. Klewes, L., and Prehm, P. (1994) *J. Cell. Physiol.* **160,** 539–544
76. Zhang, Y., and Derynck, R. (2000) *J. Biol. Chem.* **275,** 16979–16985
77. Ionescu, A. M., Drissi, H., Schwarz, E. M., Kato, M., Puzas, J. E., McCance, D. J., Rosier, R. N., Zuscik, M. J., and O'Keefe, R. J. (2004) *J. Cell. Physiol.* **198,** 428–440